# Nonlinear Seismic Response of Small-Scale Reinforced Concrete Shear Wall Structures

E.G. Endebrock, R.C. Dove
*Los Alamos National Laboratory, MS J576, P.O. 1663, Los Alamos, New Mexico 87545, U.S.A.*

SUMMARY

The paper describes dynamic tests on small shear wall structures. The purpose of the tests was to obtain information on the behavior of reinforced concrete structures loaded into their nonlinear range.

The small shear wall structures were subjected to classical sine-sweep vibration tests and to generated earthquake records. The results indicate that sine-sweep tests on degrading structures do not yield useful results because of fatigue effects and because steady-state motions cannot be achieved; however, the earthquake tests did yield useful information.

From the earthquake tests results, responses were obtained that were plotted on computed linear and nonlinear non-dimensionalized response spectra. For loading within the linear range, the data indicates that the equivalent viscous damping for the test structures is about 12.5%. The test results also indicate that, in general, manipulation of the viscous damping coefficient cannot be used to predict nonlinear behavior. The more significant observation was that the effective stiffness of the shear wall structures, as determined from the dynamic tests, was only about 1/5-1/7 of the stiffness calculated using standard calculation methods.

## 1. Introduction

The information presented here was obtained through a program that was established to address the U.S. Nuclear Regulatory Commission licensing issue: can existing facilities continue to operate in light of more demanding criteria (and potential changes in operating modes) than were considered in the initial design? A test program was designed to increase the understanding of the behavior of Category-I structures (otner tnan the containment) subjected to earthquake loads larger than the base loads. The seismic loadings that produced nonlinear behavior were of primary interest. This report describes the dynamic tests that were conducted on small isolated shear wall structures subjected to dynamic loadings.

## 2. Description of Test Structure

Previous information on the dynamic testing of reinforced concrete shear wall, one of the principal structural elements of a Category-I building, is limited; therefore, the shear wall was selected for testing. Because of limited test facility loading capacities and the desire to fail the test structures, it was necessary to use small-sized shear wall test structures. A 25 mm (1 in.) wall thickness was selected (actual building wall thicknesses range from 0.46-1.2 m (18-48 in.). The length of the test section was 0.46 m (18 in.) and the length-to-height ratio was 2.5. The shear wall test structure and reinforcement details are shown in Fig. 1.

The shear wall reinforcing consisted of a layer of 12.5 mm (0.5 in.) mesh hail screen located near each wall surface. The reinforcement ratio was 0.28% each way in each face. Anchorage was sufficient to develop the full strength of the screen wires. Threaded rods were placed near the wall ends to provide flexural reinforcement (Fig. 1). The microconcrete compressive strength ranged from 41.4-48.3 MPa (6000-7000 psi) with tensile strengths of approximately 10% of the compressive strength. The modulus of elasticity was about 20.7 GPa ($3.0 \times 10^6$ psi).

## 3. Vibration Tests

Five shear wall structures were subjected to sine-sweep tests. The shear wall structures were mounted on a horizontal slip table driven by an 89 KN (20,000 lb force) electrodynamic shaker. Added mass consisted of five steel plates with a total mass of 136 kg (300 lbs). The primary data recorded were the horizontal base acceleration (input) and horizontal accelerations of the mass (response). Ouring the sine-sweep tests, the shaker was controlled on the response. Ouring each test, the response acceleration was increased with each successive test until failure occurred. The usual absolute acceleration transmissibility curves for each sine-sweep test of a particular shear wall structure are shown in Fig. 2. Failure occurred whenever a wall-to-base interface flexural crack formed at each end and then propagated until the cross section had insufficient strength to resist the shear forces.

Transmissibility curves show how effective natural frequency and equivalent viscous damping are influenced by the response acceleration level. Effective natural frequencies decrease as the response acceleration increases. The equivalent visous damping increased in some cases and decreased in others; hence, no conclusion could be stated.

The major conclusion derived from the sine-sweep tests was that classical vibration tests yield little useful information relating to predicting response of degrading structures. Fatigue failure likely occurs because the test structures are subjected to hundreds

of thousands of load reversals before final failure. Classical vibration test solutions depend upon steady-state responses, and for degrading structures, it is doubtful that steady-state can be achieved.

4. Simulated Seismic Tests

In another test series, both one- and two-story isolated shear wall structures were subjected to simulated seismic base excitation. The test results are presented in terms of the input and response accelerations ($\ddot{Y}$ and $\ddot{X}$).

The basic accelerogram used in these tests was one that had been constructed so as to envelope the NRC Horizontal Design Response Spectrum. This accelerogram, called EE1, and its linear response spectrum are shown in Fig. 3. This 'real' time eartnquake signal was then frequency (or time) scaled to produce four accelerograms with tne appropriate frequency content for tne small structures being tested.

Time Scales ($N_t$) used were:

4.1 $N_t$ = 4.96; this signal, designated EE1 x 5, is identical in shape to the real time signal, Fig. 3a, but with a duration of 2.42s, i.e., 12/4.96s. Tne frequency spectra (response, Fourier, etc.) is 'up' snifted.

4.2 $N_t$ = 10.0; designated as EE1 x 10, duration of 1.20 s, and naving a frequency content 'up' shifted by a factor of 10.

4.3 $N_t$ = 19.85; designated as EE1 x 20, duration of 0.61 s, and having a frequency content 'up' shifted by a factor of 19.85.

4.4 $N_t$ = 53.0; designated as EE1 x 50, duration of 0.23 s, and naving a frequency content 'up' shifted by a factor of 53.

A typical test sequence is outlined below.

4.5 A structure is mounted on tne snaker. Accelerometers and displacement gages are mounted and calibrated. All calibration data is recorded on tape.

4.6 The desired test signal (EE1 x 5, EE1 x 10, EE1 x 20, or EE1 x 50) and the peak input acceleration ($\ddot{Y}_{pk}$) are selected.

4.7 The shaker is driven with a wide band, low amplitude signal selected to excite all major resonances in the test structure and the shaker system. This test is referred to as the system self test and is necessary since tne shaker control system must compute an appropriate transfer function before it can successfully execute the desired command signal (EE1 x 5, etc.). Data are tape recorded from all transducers (accelerometers and displacement gages) during this system self test.

4.8 The shaker is driven to produce tne desired accelerogram (EE1 x 5, etc.). Data are tape recorded.

4.9 After visual inspection of tne structure and preliminary analysis of the data the structure may be removed or, if there is no apparent damage, the structure may be retested using any of tne four accelerograms at any desired amplitude level. A damaged structure may also be retested after damage is noted in order to investigate the effect of a seismic event on a previously damaged structure.

5. Test Results

Immediately following eacn test, the accelerometer data [response acceleration ($\ddot{X}$) and input acceleration ($\ddot{Y}$)] were analyzed. Transfer functions were used to determine resonant frequencies. Figure 4 shows tne transfer function plot from the first system self

test conducted on a single-story structure (No. 23). From Fig. 4, we conclude that the modal frequency for this structure in the 'new' condition is approximately 115 Hz.

Figure 5 shows the transfer function plot from a test in which the same structure was subjected to the simulated earthquake EEl x 50 with a peak acceleration level ($\ddot{Y}_{pk}$) of 0.94 g's. When subjected to this earthquake, the first mode frequency is slightly lower than was indicated from the low level broad band test in the 'new' condition.

Inspection of this model following the test failed to reveal any visible cracks. By repeating the system self test, it was determined that the natural frequency had been slightly reduced from 115 to 108 Hz.

This model was retested several times by subjecting it to earthquake signals with progressively higher peak acceleration levels. Figure 6 shows the transfer function plot from a test in which this model was subjected to the EEl x 50 earthquake with a peak acceleration level of 13.8 g's. The natural frequency is reduced to 58 Hz. Following this test, inspection revealed a few visible cracks. When the system self test was repeated, the natural frequency had decreased to 100 Hz. A summary of the tests on Model 23 is given in Table I.

The standard linear response spectrum diagram for any given earthquake can be made non-dimensional by plotting the appropriate response ratio, for example, $\ddot{X}_{pk}/\ddot{Y}_{pk}$, vs the ratio of the structure's natural frequency ($\omega$) to the characteristic earthquake frequency ($\dot{\theta}$). The value of $\dot{\theta}$ was taken as the frequency at which the power spectral density plot of this earthquake signal peaks. The measured response ratios obtained from the tests on Model 23 are plotted on Fig. 7. From this plot we observe that if a linear response spectrum were used to predict the response, an equivalent viscous damping ratio ($\zeta$) of at least 12.5% would be appropriate. Also, when these structures have been loaded into the nonlinear, inelastic region, the response is reduced to values even lower than predicted using this relatively large amount of damping.

The level of input acceleration required to produce nonlinear response and the relative degree of nonlinearity associated with a given input acceleration level can be accomplished by monitoring effective resonant frequency shifts that occur when the input acceleration is increased. The data was therefore analyzed in the frequency domain.

Experimental acceleration response ratios, both for linear and nonlinear loading, are shown in Fig. 7. To aid in explaining nonlinear behavior, the authors computed nonlinear response spectra based on the assumption that reinforced concrete structures behave as softening, hysteretic systems [1]. The results of the earthquake seismic tests that were carried into the nonlinear region supports the results predicted by the proposed nonlinear spectrum. The manner in which response spectra change as a structure is loaded into its nonlinear range is illustrated in Fig. 8. In the nonlinear range, the acceleration response ratios ($\ddot{X}_{PK}/\ddot{Y}_{PK}$) decreases with increasing input acceleration level in a manner that cannot be explained by increasing equivalent damping.

After each test, the structure was visually inspected for signs of damage. In all cases, a noticeable change in effective stiffness had occurred before any visible cracking occurred; therefore, visual inspection of reinforced concrete structures may not be adequate to determine whether or not a structure has been loaded into its nonlinear response region by a past earthquake.

## 6. Conclusions

Several conclusion were drawn from the dynamic tests on small sized isolated shear wall structures. They are:

1. classical vibration tests that depend upon steady-state motions are not effective in determining the behavior of nonlinear, degrading structures. Transient signals should be used;
2. the effective stiffness of the structures when subjected to dynamic loading was only 1/5 to 1/7 of the stiffness computed using standard engineering practice;
3. the test results indicated that considerable degradation of effective stiffness had occurred before significant visible concrete cracking occurred;
4. the equivalent viscous system damping for the linear range of behavior was in excess of 10%; and
5. adjusting the equivalent viscous damping is not valid for predicting nonlinear behavior over a wide frequency band.

## Reference

[1] E. Endebrock and R. Dove, "Seismic Response of Nonlinear Systems," Los Alamos National Laboratory report LA-8981-MS, NUREG/CR-2310 (September 1981).

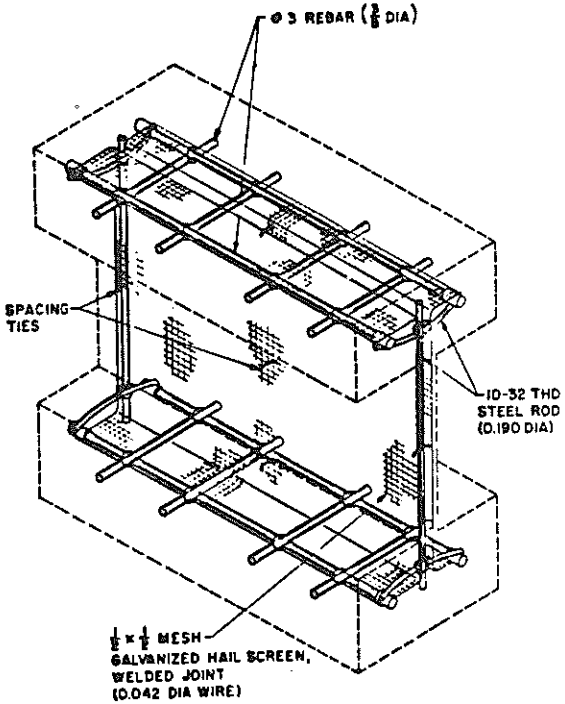


Notes:

1. Through holes in top and bottom flanges not shown.
2. Group II (specimens No. 4 and No. 5) as shown in figure.
3. Group I (specimens No. 1, 2, and 3) differ as follows: two, 10-32 steel rods at each end of web and double layer of mesh at the web/flange joints.

FIG. 1. REINFORCEMENT DETAILS.

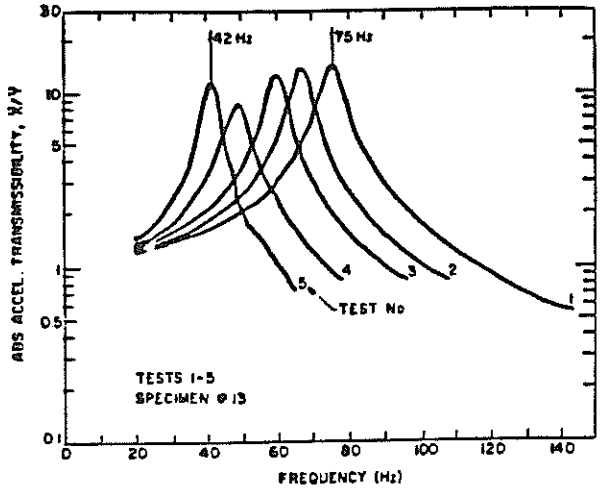


Fig. 2. TRANSMISSIBILITY, SPECIMEN NO. 13.

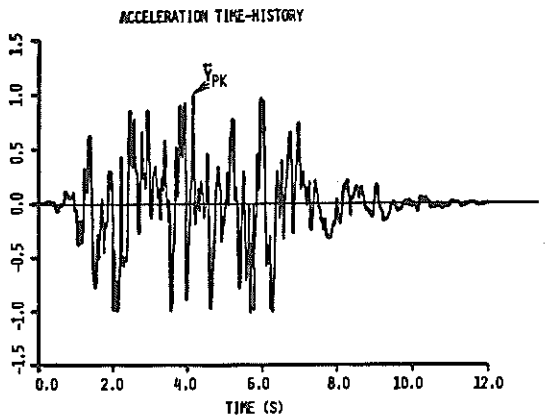


FIG. 3A. EE1 ACCELEROGRAM.

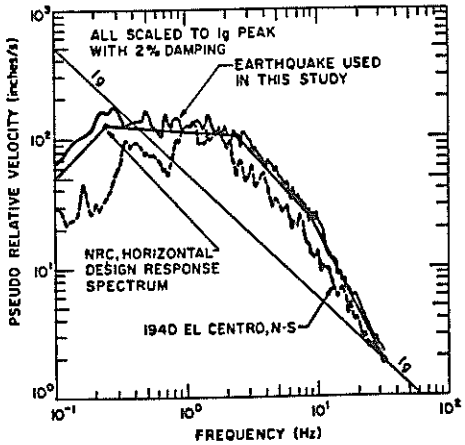


FIG. 3B. LINEAR RESPONSE FOR EE1. ACCELEROGRAM.

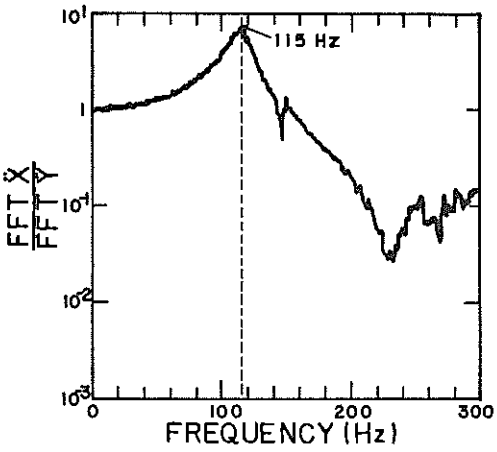


FIG. 4. TRANSFER FUNCTION, FIRST SYSTEM SELF TEST, MODEL 23.

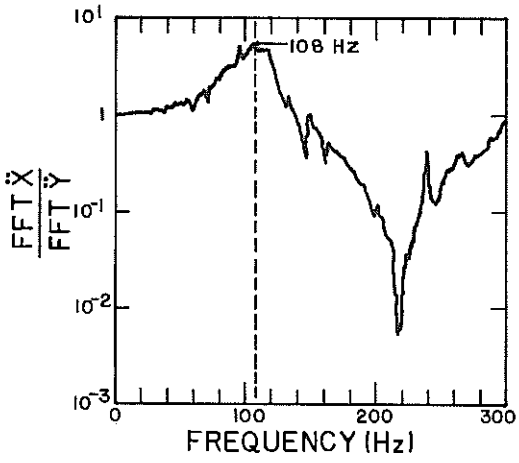


FIG. 5. TRANSFER FUNCTION, EE1 x 5D, $\ddot{Y}_{PK}$ = 0.94 g's.

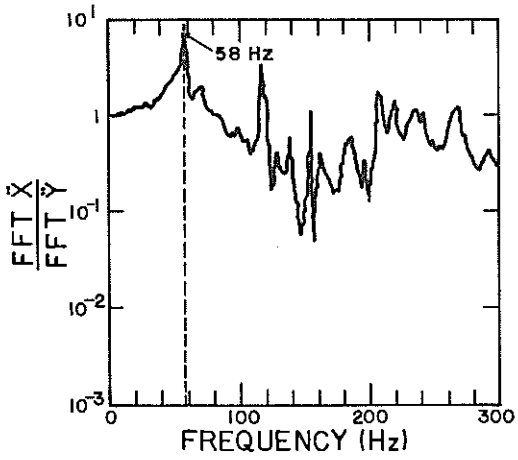


FIG. 6. TRANSFER FUNCTION, EE1 x 50, $\ddot{Y}_{PK}$ = 13.8 g's, MODEL 23.

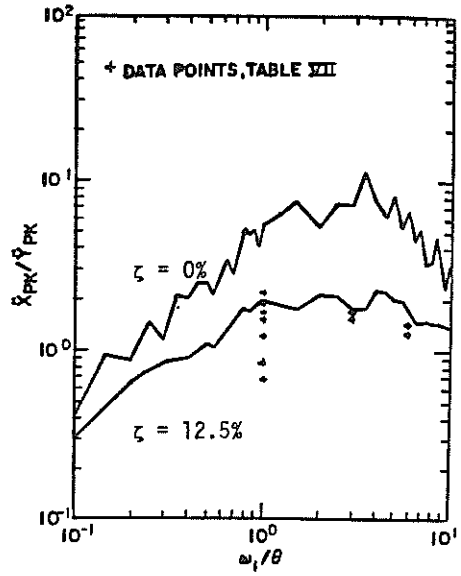


FIG. 7. EXPERIMENTALLY DETERMINED RESPONSE SPECTRUM, MODEL 23.

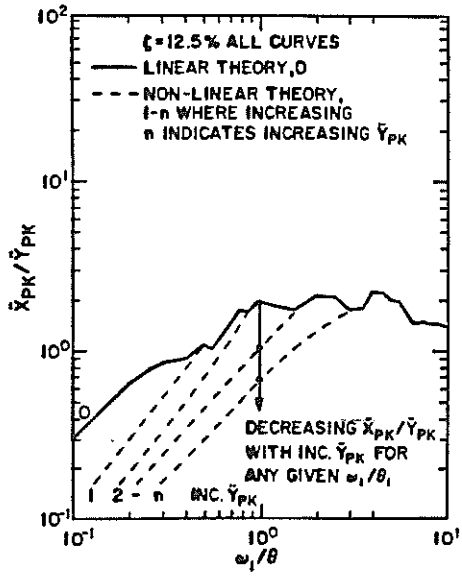


FIG. 8. NONLINEAR EFFECTS.

TABLE I

MODEL 23 - SIMULATED SEISMIC TEST RESULTS

| Test Designation | Peak Input Acceleration | Specimen Resonant Frequency[a] | | | Acceleration Response Ratio | Relative Displacement Maximum | $\omega_1/\theta$[b] | K eff ($lb/in.x10^6$)[c] | |
|---|---|---|---|---|---|---|---|---|---|
| | | Pretest | During Test | Post Test | | | | $K_1$,eff | $K_e$,eff |
| | $\ddot{Y}_{PK}$(g) | $f_1$(Hz) | $f_e$(Hz) | $f_p$(Hz) | $\ddot{X}_{PK}/\ddot{Y}_{PK}$ | u($in.x10^{-3}$) | $2\pi f_1/\theta$ | | |
| EE1 x 5 | 0.34 | 115 | 115 | 115 | 1.51 | 1.2 | 12.2 | 0.46 | 0.46 |
| EE1 x 10 | 0.69 | 115 | 115 | 115 | 1.37 | 1.4 | 6.05 | 0.46 | 0.46 |
| EE1 x 10 | 1.21 | 108 | 112 | 112 | 1.27 | 1.5 | 5.68 | 0.41 | 0.44 |
| EE1 x 10 | 3.46 | 108 | 110 | 112 | 1.26 | 3.9 | 5.68 | 0.41 | 0.42 |
| EE1 x 20 | 0.95 | 112 | 108 | 112 | 1.62 | 2.6 | 2.97 | 0.44 | 0.41 |
| EEL x 20 | 1.88 | 112 | 106 | 108 | 1.84 | 5.3 | 2.97 | 0.44 | 0.39 |
| EE1 x 20 | 2.70 | 115 | 99 | 112 | 1.85 | 6.5 | 3.05 | 0.46 | 0.34 |
| EE1 x 20 | 4.10 | 112 | 93 | 102 | 1.60 | 6.7 | 2.97 | 0.44 | 0.30 |
| EE1 x 50 | 0.46 | 115 | 115 | 115 | 2.26 | 1.7 | 1.14 | 0.46 | 0.46 |
| EE1 x 50 | 0.54 | 115 | 115 | 108 | 1.92 | 1.7 | 1.14 | 0.46 | 0.46 |
| EE1 x 50 | 0.94 | 112 | 108 | 108 | 1.64 | 2.6 | 1.11 | 0.44 | 0.41 |
| EE1 x 50 | 2.34 | 108 | 107 | 115 | 1.89 | 4.9 | 1.07 | 0.41 | 0.40 |
| EE1 x 50 | 4.77 | 102 | 96 | 110 | 1.46 | 8.1 | 1.10 | 0.36 | 0.32 |
| EE1 x 50 | 10.7 | 110 | 73 | 105 | 1.17 | 3.4 | 1.09 | 0.42 | 0.19 |
| EE1 x 50 | 13.8 | 105 | 58 | 100 | 0.86 | 3.7 | 1.04 | 0.38 | 0.12 |
| EE1 x 50 | 20.8 | 100 | 58 | 90 | 0.64 | 6.2 | 0.99 | 0.35 | 0.12 |

Notes:

a. $f_1$ is determined by the low level, broad band system self test that precedes each simulated seismic test, $f_e$ is the effective resonant frequency during the test; taken as the frequency at which the transfer function (FFT X/FFT Y) is maximum. $f_p$ is determined from the system self test following each simulated seismic test.

b. For a given test signal, $\theta = \theta$ is the value of the arbitrarily selected characteristic frequency of the original earthquake ($2\pi$ x 1.9 = 11.94 radians/s) times the factor by which the original signal has been frequency scaled, $N_\theta$. Hence for the EE1 x 5 test $\theta$ = 11.94 x 4.96 = 59.2 rad/s since the EE1 x 5 test signal has been frequency scaled by a factor of 4.96.

c. The effective stiffness (K eff) is computed as $K_1$, eff = $(2\pi f_1)^2 M = (2\pi f_1)^2$ x (300+40)/386 and $K_e$, eff = $(2\pi f_e)^2$ x (300+40)/386.